Article

Midpoint Potentials of Hemes *a* and *a*$_3$ in the Quinol Oxidase from *Acidianus ambivalens* are Inverted

Smilja Todorovic, Manuela M. Pereira, Tiago M. Bandeiras, Miguel Teixeira, Peter Hildebrandt, and Daniel H. Murgida

J. Am. Chem. Soc., **2005**, 127 (39), 13561-13566• DOI: 10.1021/ja052921l • Publication Date (Web): 09 September 2005

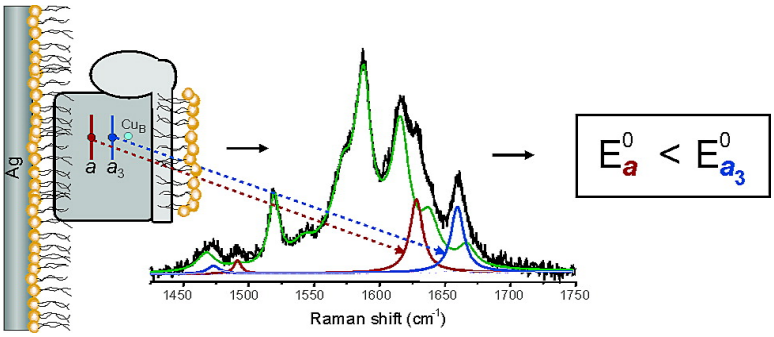

More About This Article

Additional resources and features associated with this article are available within the HTML version:

- Supporting Information
- Links to the 3 articles that cite this article, as of the time of this article download
- Access to high resolution figures
- Links to articles and content related to this article
- Copyright permission to reproduce figures and/or text from this article

View the Full Text HTML

J|A|C|S
ARTICLES
Published on Web 09/09/2005

Midpoint Potentials of Hemes *a* and a_3 in the Quinol Oxidase from *Acidianus ambivalens* are Inverted

Smilja Todorovic,[†] Manuela M. Pereira,[†] Tiago M. Bandeiras,[†] Miguel Teixeira,[†] Peter Hildebrandt,[†,‡] and Daniel H. Murgida*[,†,‡]

Contribution from the Instituto de Tecnologia Química e Biológica, Universidade Nova de Lisboa, Apartado 127, 2781-901 Oeiras, Portugal, and Max-Volmer-Laboratorium für Biophysikalische Chemie, Institut für Chemie, Technische Universität Berlin, Sekr. PC14, Strasse des 17. Juni 135, D-10623 Berlin, Germany

Received May 4, 2005; E-mail: dh.murgida@tu-berlin.de

Abstract: The aa_3 type B oxygen reductase from the thermophilic archaeon *Acidianus ambivalens* (QO) was immobilized on silver electrodes and studied by potential-dependent surface-enhanced resonance Raman (SERR) spectroscopy. The immobilized enzyme retains the native structure at the level of the heme pockets and exhibits reversible electrochemistry. From the potential dependence of specific spectral marker bands, the midpoint potentials of hemes *a* and a_3 were unambiguously determined for the first time, being 320 ± 20 mV for the former and 390 ± 20 mV for the latter. Both hemes could be treated as independent one-electron Nernstian redox couples, indicating that the interaction potential is smaller than 50 mV. The reversed order of the midpoint potentials compared to those of type A (mitochondrial-like) oxidases, as well as the lack of substantial Coulombic interactions, suggests a different mechanism of electroprotonic energy transduction. In contrast to type A enzymes, $a-a_3$ intraprotein electron transfer in QO is already guaranteed by the order of the midpoint potentials at the onset of enzyme reduction and, therefore, does not require a complex network of cooperativities to ensure exergonicity. In the immobilized state, conformational transitions of the QO a_3-Cu_B active site, which are believed to be essential for proton translocation, are drastically slowed compared to those in solution. We ascribe this finding to the effect of the interfacial electric field, which is of the same order of magnitude as in biological membranes. These results suggest that the membrane potential may play an active role in the regulation of the enzymatic activity of QO.

Introduction

Acidianus ambivalens is a thermoacidophilic archaeon with optimum growth temperature of 81 °C and pH 2. Its respiratory chain has been the subject of several studies with special attention to its oxygen reductase, the aa_3 quinol oxidase (QO).[1,2] This type B oxygen reductase[3] belongs to the superfamily of heme−copper terminal enzymes in respiratory chains that transfer electrons from reducing substrates, such as cytochrome *c* or quinols, to molecular oxygen, producing water and uphill transmembrane proton translocation.

Acidianus ambivalens oxygen reductase contains a heme *a* redox center and a heme a_3-Cu_B binuclear (oxygen binding) catalytic center.[4] Like all other quinol oxidases, it lacks the binuclear Cu_A center, which is the primary electron acceptor in oxidases receiving electrons from soluble metallo-proteins.[5,6] Instead, a loosely bound benzothiophene (caldariella) quinone, which is lost during purification, is believed to act as the electron entry site.[6] Binding properties of QO at the a_3-Cu_B center also differ significantly from those of mitochondrial-like oxygen reductases (type A enzymes).[6]

Das et al.[1,4] have characterized *A. ambivalens* aa_3 QO by resonance Raman (RR) spectroscopy. In general terms, the RR spectra of QO match very well those from other aa_3 oxidases and are consistent with a six-coordinated low-spin heme *a* and a high-spin heme a_3, which in this enzyme lacks the bridging ligand (five-coordinated). The positions of the formyl stretching modes ($\nu_{C=O}$), however, indicate differences of polarity and hydrogen bonding for both hemes with respect to bovine cytochrome *c* oxidase (Cox). Furthermore, upon reduction, the $\nu_{C=O}$ band of heme a_3 undergoes a time-dependent frequency shift, which was interpreted in terms of slow conformational changes that involve proton exchange.[1,4] Thus, although QO bears similarities with the better understood type A oxygen reductases, it also shows very distinct features that may be characteristic of the B-type enzymes.

[†] Universidade Nova de Lisboa.
[‡] Technische Universität Berlin.

(1) Das, T. K.; Gomes, C. M.; Teixeira, M.; Rousseau, D. L. *Proc. Natl. Acad. Sci. U.S.A.* **1999**, *96*, 9591−9596.
(2) Purschke, W. G.; Schmidt, C. L.; Petersen, A.; Shafer, G. *J. Bacteriol.* **1996**, *179*, 1344−1353.
(3) Pereira, M. M.; Teixeira, M. *Biochim. Biophys. Acta* **2004**, *1655*, 340−346.
(4) Das, T. K.; Gomes, C. M.; Bandeiras, T. M.; Pereira, M. M.; Teixeira, M.; Rousseau, D. L. *Biochim. Biophys. Acta* **2004**, *1655*, 306−320.
(5) Aagaard, A.; Gilderson, G.; Gomes, C. M.; Teixeira, M.; Brzezinski, P. *Biochemistry* **1999**, *38*, 10032−10041.
(6) Giuffre, A.; Gomes, C. M.; Antonini, G.; Ditri, E.; Teixeira, M.; Brunori, M. *Eur. J. Biochem.* **1997**, *250*, 383−388.

A prerequisite for understanding the functioning of oxygen reductases, in general, and of QO, in particular, is the determination of the midpoint potentials of the cofactors and the identification of their possible interactions and linkage to proton transfer processes. Previous spectrophotometric redox titrations of QO, however, yielded conflicting results with only poorly resolved transitions.[4,6] The low and high potential transitions were tentatively assigned to hemes *a* and a_3, respectively. Both transitions were found to exhibit substantial redox Bohr effects. The determination of midpoint potentials in heme−copper oxidases by spectrophotometric methods is intrinsically complicated, on one hand, due to strong overlapping of the absorption spectra of the individual hemes and, on the other hand, due to the complex cooperative effects that modulate the electroprotonic energy transduction.[7] These problems can be partially overcome by the addition of inhibitors, such as carbon monoxide and cyanide, to heme a_3.[8−11] However, the influence of these inhibitors on the midpoint and interaction potentials remains controversial. Indeed, published redox properties of oxygen reductases are often contradictory regarding both the values and the interpretation.[9,10,12−16] Despite all the uncertainties, the observed general tendency is that heme *a* possesses a higher midpoint potential than heme a_3, at the onset of the enzyme reduction.

A common feature to all forms of respiration (and photosynthesis) is the utilization of the energy provided by reducing electrons for driving vectorial transmembrane ion translocation. The energy stored in the form of a transmembrane charge gradient is later transformed to chemical energy by ATP synthase. As a result of the transmembrane charge gradient, interfacial electric fields of ca. 10^7 V/m are generated. In addition, the surface and dipole potentials of membranes can produce electric fields of up to 10^9 V/m.[17] Thus, under physiological conditions, the different components of respiratory chains (e.g., QO) exert their function under the influence of very strong electric fields. The influence of such fields on the structure and reaction dynamics of the intervening redox proteins and enzymes is still an open question. Addressing these issues requires experimental methods capable of providing simultaneous structural and dynamic information and, at the same time, delivering electric fields in the range 10^7-10^9 V/m in a controllable fashion.

Here we report a potential-dependent surface-enhanced resonance Raman (SERR) study of *A. ambivalens* aa_3 QO immobilized on silver electrodes. The method combines the ability of Raman spectroscopy to distinguish redox, coordination, and spin states of hemes with the high sensitivity and selectivity provided by the resonance and surface-enhancement effects, which allow for the detection of individual heme groups solely of the adsorbed QO. This approach has been successfully applied to the study of electron transfer and conformational equilibria and dynamics of monoheme[18−21] and multiheme[22,23] redox proteins and enzymes.[24,25] It has been shown that electrochemical interfaces are useful model systems for mimicking some basic features of biological interfaces, namely, the interfacial electric field at biological membranes.[21]

The present study provides, for the first time, an unambiguous determination of the redox properties of the two heme groups in QO. It is shown that the two redox centers are largely uncoupled and exhibit reversed midpoint potentials with respect to type A enzymes. In addition, it was found that electric fields of biologically relevant magnitude have a substantial effect on redox-linked conformational changes that occur at the level of the catalytic site of the enzyme.

Materials and Methods

Protein Sample. The aa_3 oxygen reductase from *Acidianus ambivalens* was purified as described elsewhere.[26,27] For SERR experiments, an aliquot of the enzyme was added to an electrochemical cell containing oxygen-free buffer solution (40 mM phosphate buffer, pH 6.5, with 0.1% *n*-dodecyl-β-D-maltoside) to give a final concentration of ca. 0.1 μM. Before measurements, the electrochemical cell was further purged with Ar for 1 h while keeping the working electrode at −100 mV. All the potentials reported in this work refer to NHE.

RR spectra of QO were measured from a 1.5 μM solution in 40 mM phosphate buffer (pH 6.5) with 0.1% dodecyl maltoside. The RR spectrum of the fully reduced QO was obtained by chemical reduction of the enzyme with excess of sodium dithionite.

SERR and RR Experiments. Unless stated otherwise, all measurements were performed with the 413 nm excitation line of a krypton ion laser (Coherent Innova 302).

For SERR spectroscopic experiments, the laser beam was focused onto the surface of a home-built rotating Ag electrode. A detailed description of the electrochemical setup as well as of the protocol for preparing SER-active Ag electrodes is given elsewhere.[18] The scattered light was collected in a backscattering geometry using a confocal microscope coupled to a single stage spectrograph (Jobin Yvon XY) equipped with a 1800 l/mm grating and liquid nitrogen cooled back-illuminated CCD detector. Elastic scattering and reflected light were rejected with notch filters. To avoid laser-induced photoreduction of the adsorbed protein, the exposure was minimized by using a long working distance (2 cm) and low numerical aperture objective (20X; na = 0.35), a laser power lower than 0.3 mW, a rotational speed of the working electrode of ca. 5 Hz, and short accumulation times (ca. 10 s). SERR spectra with good S/N ratio were obtained by acquisition and addition of 4−6 spectra collected under the same experimental conditions but from different spots on the electrode. The spectral bandwidth was ca. 2 cm^{-1} and the increment per data point 0.47 cm^{-1}.

(7) Xavier, A. V. *Biochim. Biophys. Acta* **2004**, *1658*, 23−30.
(8) Junemann, S.; Meunier, B.; Gennis, R. B.; Rich, P. R. *Biochemistry* **1997**, *36*, 14456−14464.
(9) Kojima, N.; Palmer, G. *J. Biol. Chem.* **1983**, *258*, 14908−14913.
(10) Meunier, B.; Ortwein, C.; Brandt, U.; Rich, P. R. *Biochem. J.* **1998**, *330*, 1197−1200.
(11) Moody, A. J.; Rich, P. R. *Biochim. Biophys. Acta* **1990**, *1015*, 205−215.
(12) Anemuller, S.; Schafer, G. *FEBS Lett.* **1989**, *244*, 451−455.
(13) Blair, D. F.; Ellis, W. R.; Wang, H.; Gray, H. B.; Chen, S. I. *J. Biol. Chem.* **1986**, *261*, 11524−11537.
(14) Hellwig, P.; Grzybek, S.; Behr, J.; Ludwig, B.; Michel, H.; Mäntele, W. *Biochemistry* **1999**, *38*, 1685−1694.
(15) Mitchell, R.; Mitchell, P.; Rich, P. R. *FEBS Lett.* **1991**, *280*, 321−324.
(16) Salerno, J. C.; Bolgiano, B.; Poole, R. K.; Gennis, R. B.; Ingledew, W. J. *J. Biol. Chem.* **1990**, *265*, 4364−4368.
(17) Clarke, R. J. *Adv. Colloid Interface Sci.* **2001**, *89*, 263−281.
(18) Murgida, D. H.; Hildebrandt, P. *J. Phys. Chem. B* **2001**, *105*, 1578−1586.
(19) Murgida, D. H.; Hildebrandt, P. *J. Am. Chem. Soc.* **2001**, *123*, 4062−4068.
(20) Murgida, D. H.; Hildebrandt, P. *J. Phys. Chem. B* **2002**, *106*, 12814−12819.
(21) Murgida, D. H.; Hildebrandt, P. *Acc. Chem. Res.* **2004**, *37*, 854−861.
(22) Rivas, L.; Soares, C. M.; Baptista, A. M.; Simaan, J.; Di Paolo, R.; Murgida, D. H.; Hildebrandt, P. *Biophys. J.* **2005**, *88*, 4188−4199.
(23) Simaan, A. J.; Murgida, D. H.; Hildebrandt, P. *Biopolymers* **2002**, *67*, 331−334.
(24) Friedrich, M. G.; Gie, F.; Naumann, R.; Knoll, W.; Ataka, K.; Heberle, J.; Hrabakova, J.; Murgida, D. H.; Hildebrant, P. *Chem. Commun.* **2004**, *21*, 2376−2377.
(25) Todorovic, S.; Jung, C.; Hildebrandt, P.; Murgida, D. H. Unpublished work.
(26) Gomes, C. M.; Backgren, C.; Teixeira, M.; Puustinen, A.; Verkhovskaya, M. L.; Wikstrom, M.; Verkhovsky, M. I. *FEBS Lett.* **2001**, *497*, 159−164.
(27) Teixeira, M.; Batista, R.; Campos, A. P.; Gomes, C. M.; Mendes, J.; Pacheco, I.; Anemuller, S.; Hagen, W. R. *Eur. J. Biochem.* **1995**, *227*, 2039−2045.

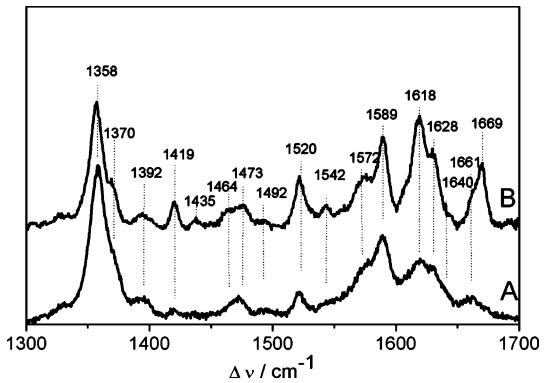

Figure 1. (A) SERR spectrum of adsorbed QO at a potential of −403 mV. (B) RR spectrum of QO in solution reduced with excess of dithionite. Conditions are as described in the Materials and Methods.

The spectral calibration and linearity control of the spectrometer was performed with a Hg/Ne calibration lamp (Oriel).

Spectroelectrochemical titrations were performed in the potential range from −403 to + 337 mV in ca. 50 mV steps under anaerobic conditions. After each change of potential, the system was allowed to equilibrate for at least 30 min before the SERR measurement.

RR spectra were measured from solutions in a rotating quartz cuvette using a laser power of ca. 2.8 mW. The spectra displayed in this work represent the average of 20 spectra each measured with an accumulation time of 30 s. All other conditions were the same as used for the SERR measurements.

After background subtraction, the SERR spectra were subjected to a component analysis in which the spectra of the individual species were fitted to the measured spectra.[28]

Results and Discussion

Structural Integrity of the Immobilized Enzyme. Quinol oxidase was immobilized on Ag electrodes by spontaneous adsorption of the detergent-solubilized enzyme. At potentials positive to the potential of zero charge ($E_{pzc} \approx -0.8$ V), the metal surface carries an excess of negative charges due to specifically adsorbed phosphate anions. Adsorption of QO to such surfaces was probed by SERR spectroscopy, which gives relatively strong signals that display the characteristic features of a heme protein (Figure 1A).

By comparing the intensities of the SERR spectrum measured at −403 mV and the RR spectrum of the dithionite-reduced enzyme (Figure 1B), and taking into account the different experimental conditions, we estimate a lower limit for the surface enhancement factor of ca. 1000. In agreement with this estimation, no signal could be detected upon slight defocusing of the laser beam from the electrode surface. Thus, it can be safely concluded that under the present conditions, SERR measurements selectively probe the heme groups of solely adsorbed species without interference of molecules from the bulk solution.

Previous studies have shown that the direct adsorption of heme proteins to bare metal surfaces can induce alterations of the protein structure, which in turn may result in the loss or exchange of the iron axial ligands.[21,29] These changes are reflected in the SERR spectra by large shifts of the high-frequency bands (1300−1700 cm^{-1}), which are sensitive reporters of the redox, coordination, and spin state of the heme iron.[21,29]

Since the RR and SERR spectra of reduced QO in solution and in the adsorbed state, respectively, display identical band positions (Figure 1 and Table 1), we conclude that the native protein structure, at least at the heme sites, is not affected upon immobilization. Most likely, adsorption of the protein to the hydrophilic surface of the phosphate-coated electrode occurs without displacement of the detergent, which then provides a biocompatible interface. This conclusion is supported by the fact that, upon immersion of the electrode into a protein-free buffer solution containing *n*-dodecyl-*β*-D-maltoside, a SER signal at 2950 cm^{-1} attributable to the C−H stretching modes of the detergent becomes clearly detectable with 514 nm excitation (data not shown).

We note, however, some variations of the relative band intensities between the RR and SERR spectra (Figure 1). These differences are attributed to the orientation dependence of the SERR effect, which may cause different enhancements, not only for the vibrational modes of heme *a* versus heme a_3 but also for modes of different symmetry of each heme.[30]

In a recent study,[24] a His-tagged Cox was immobilized within a lipid bilayer onto a Ni−NTA-coated Ag electrode. In this case, in which the physiological environment of the membrane protein is closely mimicked and direct interaction of the protein with the metal surface is avoided, the SERR spectra also display the same band frequencies, but slightly different relative intensities as compared to those of the RR spectra.

The assignment of vibrational modes in aa_3 oxygen reductases is well established.[1,31−35] Upon Soret excitation, the high-frequency region (1300−1700 cm^{-1}) displays the heme *a* and heme a_3 skeletal vibrational modes as well as the stretching modes of the vinyl and formyl substituents. Specifically, the formyl stretching modes ($\nu_{C=O}$) are particularly sensitive to the immediate heme environment, and their positions can be taken as an indication for the polarity and hydrogen-bonding characteristics of the heme pocket in the vicinity of the substituents.[4,32,33] This sensitivity is illustrated by the RR spectrum of the dithionite-reduced QO, which in the equilibrium conditions displays a strong band and a shoulder at 1669 and 1661 cm^{-1}, respectively. Both bands have been assigned to the $\nu_{C=O}$ mode of two heme a_3 conformations that differ with respect to the formyl environment.[1,4] Immediately after chemical reduction of the enzyme, the band at 1661 cm^{-1} dominates this spectral region, but it gets subsequently replaced by the 1669 cm^{-1} band. The kinetics of the process is temperature- and pH-dependent and exhibits a substantial H/D isotope effect, indicating a conformational transition at the level of the heme a_3−Cu_B center, which involves proton transfer and a rearrangement of the hydrogen-bonding network.

The SERR spectrum of the reduced QO only displays the band at 1661 cm^{-1}, and no time-dependent increase of intensity at 1669 cm^{-1} is noted within 30 min. This finding implies that

(28) Döpner, S.; Hildebrandt, P.; Mauk, A. G.; Lenk, H.; Stempfle, W. *Spectrochim. Acta A-Mol. Biomol. Spectrosc.* **1996**, *52*, 573−584.
(29) Wackerbarth, H.; Hildebrandt, P. *ChemPhysChem* **2003**, *4*, 714−724.
(30) Kanger, J. S.; Otto, C. *Appl. Spectrosc.* **2003**, *57*, 1487−1493.
(31) Argade, P. V.; Ching, Y.; Rousseau, D. L. *Biophys. J.* **1986**, *50*, 613−620.
(32) Heibel, G. E.; Hildebrant, P.; Ludwig, B.; Steinrücke, P.; Soulimane, T.; Buse, G. *Biochemistry* **1993**, *32*, 10866−10877.
(33) Heibel, G. E.; Anzenbacher, P.; Hildebrant, P.; Schäfer, G. *Biochemistry* **1993**, *32*, 10878−10884.
(34) Hildebrant, P.; Vanhecke, F.; Buse, G.; Soulimane, T.; Mauk, G. *Biochemistry* **1993**, *32*, 10912−10922.
(35) Pinakoulaki, E.; Pfitzner, U.; Ludwig, B.; Varotsis, C. *J. Biol. Chem.* **2002**, *277*, 13563−13568.

Table 1. Assignment of the Vibrational Modes of the RR and SERR Spectra of Oxidized and Reduced aa_3 Quinol Oxidase from *A. ambivalens*

	Reduced QO RR		Reduced QO SERR[b]		Oxidized QO RR		Oxidized QO SERR[b]	
mode[a]	*a*	a_3	*a*	a_3	*a*	a_3	*a*	a_3
$\nu_{C=O}$	1628	1661/1669	1628 (5.6/11.9)	1661 (8.4/11.9)	1653	1676	1653 (1.8/14.2)	1676 (0.3/14.0)
$\nu_{C=C}$	1618		1618		1620		1620	
ν_{10}	1640		1640		1640		1640	
ν_2	1589	1572	1589	1572	1589	1572	1589	1572
ν_{37}	1572		1572		1572		1572	
ν_{11}	1520		1520					
ν_3	1492	1473	1492 (1.0/9.8)	1471 (1.0/11.5)	1503	1480	1502 (1.0/14.6)	1478 (1.0/14.9)
ν_4	1358		1358		1370		1370	
ν_{28}	1464		1464		1476		1467	

[a] Assignment adopted from refs 1 and 4. [b] The relative intensities and widths, respectively, of the bands used for quantitative component analysis (vide infra) are indicated in parentheses.

the redox-linked conformational transition of the heme a_3 is blocked or at least drastically slowed in the immobilized QO.

The effect can be attributed to the interfacial electric field strength at the electrode that may vary between 10^8 and 10^9 V/m. Such fields are sufficiently strong to perturb acid−base equilibria as well as proton and electron transfer kinetics,[21,36−38] and thus may also modulate the proton-coupled conformational equilibrium of the heme a_3 formyl substituent. Since this conformational transition has been suggested to constitute a crucial step in the redox-coupled proton pumping activity of QO,[1,4] the present results imply that the electric fields may modulate the proton translocation through the protein. It is possible that, during aerobic respiration, the membrane potential generated by the proton pumping activity of QO becomes sufficiently large, such that the resultant electric field is able to block the elementary steps of proton translocation. In fact, electric field strengths in the interfacial regions of biological membranes are comparable to those at the electrochemical interfaces,[17,21] such that the present observation for the immobilized QO may also be relevant under physiological conditions. Such an effect would constitute the basis for a self-regulation mechanism of the proton pumping activity of the enzyme. A similar mechanism has been recently proposed for the regulation of mitochondrial respiration based on the electric field effects on conformation, redox potential, and electron transfer kinetics of cytochrome *c* (Cyt-c).[21] Furthermore, it has been shown in earlier studies that the enzymatic activity of Cox toward Cyt-c is sensitively controlled by the membrane potential.[39]

Redox Activity. Varying the electrode potential leads to distinct changes in the SERR spectra that reflect the transition between the reduced and oxidized hemes (Figure 2) and thus indicates the electrochemical activity of the immobilized QO.

The strongest band of the ferrous hemes (ν_4) is found at ca. 1360 cm^{-1}, but shifts to ca. 1370 cm^{-1} upon oxidation.[40] Thus, although the overall spectra are quite crowded and include several overlapping bands of the two hemes, a visual inspection

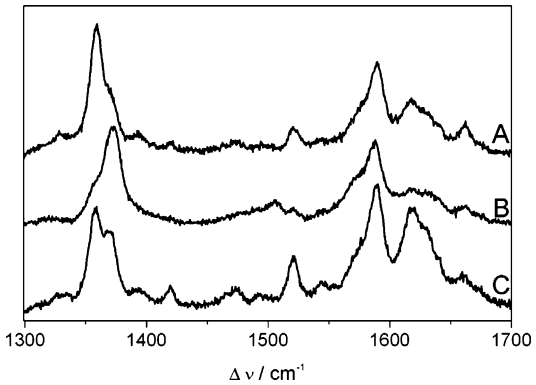

Figure 2. SERR spectra of immobilized QO recorded at (A) −103 mV, (B) 337 mV, and (C) 227 mV. Conditions are as described in the Materials and Methods.

of the ν_4 region already gives an unambiguous indication that the enzyme responds to the applied potential.

However, even at the highest potential used in this work (337 mV), the ν_4 region still exhibits a shoulder at 1360 cm^{-1} (Figure 2B), indicative of a residual contribution of ferrous hemes. Significantly more positive potentials could not be applied due to oxidation of the roughened Ag electrode.

As most heme proteins, QO can undergo laser-induced photoreduction,[4] which, in principle, might be the origin of the incomplete oxidation. Great care was taken in order to avoid this artifact by using low laser powers, a rotating electrode, and short acquisition times. The relative contribution of the reduced species to the SERR spectra shows a clear drop upon decreasing the laser power at the sample, but remains constant for powers lower than 0.5 mW. Thus, all spectra in the present study were acquired with laser powers lower than 0.3 mW. The persistence of the shoulder at 1360 cm^{-1} then indicates that at least one of the hemes possesses an intrinsically high redox potential.

Although complete oxidation could not be achieved due to the experimental constraints, the SERR spectrum recorded at 337 mV allows for identifying the marker bands of the oxidized enzyme. The band positions for the ferric state are also in very good agreement with the RR spectra of the fully oxidized QO in solution determined in the present (Table 1) and in previous work,[1,4] confirming that the immobilized protein is largely intact.

The potential-dependent SERR spectra could be quantitatively reproduced independently of the sequence of applied electrode potentials, indicating that the redox processes are fully reversible.

(36) Franzen, S.; Goldstein, R. F.; Boxer, S. G. *J. Phys. Chem.* **1990**, *94*, 5135−5149.
(37) Franzen, S.; Lao, K.; Boxer, S. G. *Chem. Phys. Lett.* **1992**, *197*, 380−388.
(38) Neumann, E. *Prog. Biophys. Mol. Biol.* **1986**, *47*, 197−231.
(39) Gregory, L.; Ferguson-Miller, S. *Biochemistry* **1989**, *28*, 2655−2662.
(40) Hildebrandt, P. In *Cytochrome c: A Multidisciplinary Approach*; Scott, R. A., Mauk, A. G., Eds.; University Science Books: Sausalito, CA, 1996; pp 285−314.

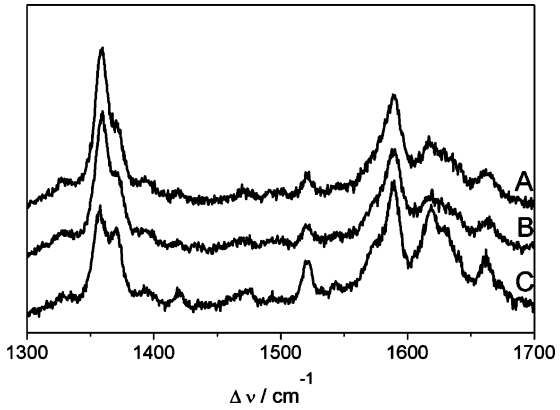

Figure 3. SERR spectra of immobilized QO recorded at variable delay times after switching the potential from −3 to +297 mV: (A) immediately, (B) 15 min, and (C) 30 min.

However, the heterogeneous electron transfer reaction was found to be very slow, as can be judged from the changes of SERR spectra recorded at different delay times after setting a certain electrode potential (Figure 3). Typically, equilibrium conditions were reached after ca. 20−30 min.

The slow electron transfer kinetics is not really surprising considering that distances from the redox centers to the electrode are relatively long and that the orientation of the immobilized QO is not necessarily optimized for electron transfer. Furthermore, this enzyme, which is isolated from a thermophilic microorganism, requires elevated temperatures for functioning at physiological turnover rates. On the other hand, the isolated protein lacks the caldariella quinone which, presumably, favors the electron entry via heme *a*, ensuring an efficient electron transfer cascade.[6] Similarly, it was shown that the bo_3 quinol oxidase from *Escherichia coli* requires a tightly bound quinol for complete oxygen reduction kinetics.[41]

Due to the large number of overlapping bands from two hemes in two oxidation states (Table 1), the determination of complete component spectra is rather complicated. Instead, we have restricted the quantitative spectral analysis to only two modes ($\nu_{C=O}$ and ν_3) that are the only unambiguous indicators for the redox states of hemes *a* and a_3. These two modes were used for defining four simplified component spectra, one for each heme in the different redox states, that contain the positions, widths, and relative intensities of the two Lorentzian bands as fixed parameters (see Table 1). A global fit to all experimental SERR spectra was achieved by varying the relative contributions of the four-component spectra, whereas for the remaining bands, only the relative intensities were treated as adjustable variables. Examples of spectra analyzed in this way are shown in Figure 4.

The relative spectral contributions I_i of the four components ($i = {}^{red}a, {}^{ox}a, {}^{red}a_3, {}^{ox}a_3$) are related to the relative concentrations c_i of these species according to

$$c_i = \frac{f_i \times I_i}{\sum_i f_i \times I_i} \qquad (1)$$

where the factors f_i are proportional to the relative reciprocal

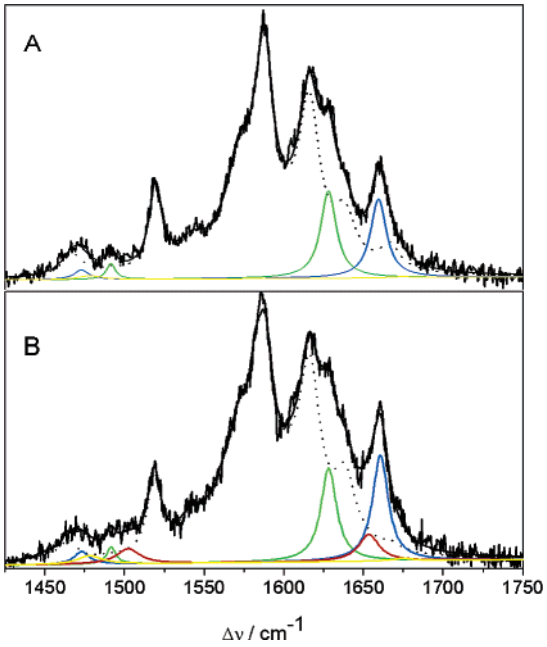

Figure 4. SERR spectra of the immobilized QO in the 1425−1750 cm^{-1} region, at (A) −3 and (B) +297 mV. The experimental and overall simulated spectra are shown in black lines. The different colors represent the individual spectral components. Green: ferrous heme *a*. Yellow: ferric heme *a*. Blue: ferrous heme a_3. Red: ferric heme a_3. Dotted black: all nonassigned bands in the 1425−1750 cm^{-1} region. The spectral parameters of the four components are summarized in Table 1.

SERR cross-sections of the species *i*. Thus, the Nernst equation for the individual redox couples can be written as

$$E = E_m - \frac{RT}{zF}\ln\frac{f_{red}}{f_{ox}} - \frac{RT}{zF}\ln\frac{I_{red}}{I_{ox}} \qquad (2)$$

where *z* is the number of transferred electrons, and *R*, *T*, and *F* have the usual meaning.

The f_{red}/f_{ox} ratios for the $\nu_{C=O}$ modes were adopted from a previous study on Cox, for which values of 2.24 and 3.02 were determined for heme *a* and a_3, respectively.[24] Note that slight variations of the f_{red}/f_{ox} ratios, which cannot be ruled out for different aa_3 oxygen reductases, do not have a significant impact on the midpoint potential, E_m.

For both, heme *a* and heme a_3, the Nernst plots display a linear behavior (Figure 5) with slopes which are very close to the theoretical value for an one electron transfer process ($z = 1$).

This finding indicates that (i) photoreduction is efficiently suppressed under the present experimental conditions, and (ii) heme *a* and heme a_3 can be treated as independent redox couples with no indication for substantial electrostatic interactions. From the dispersion of the experimental data, an upper limit of 50 mV can be estimated for the interaction potential between the two hemes. The determined midpoint potentials are 320 ± 20 and 390 ± 20 mV for hemes *a* and a_3, respectively, implying a reversed order in respect to type A enzymes. This conclusion is in agreement with an earlier tentative assignment based on spectrophotometric titrations, although the previous values were downshifted with respect to the present determination.[4,6]

Both the reversed order of the midpoint potentials and the lack of any appreciable interaction between the redox sites constitute a distinct property of *Acidianus ambivalens* QO as

(41) Puustinen, A.; Verkhovsky, M. I.; Morgan, J. E.; Belevich, N. P.; Wikström, M. *Proc. Natl. Acad. Sci. U.S.A.* **1996**, *93*, 1545−1548.

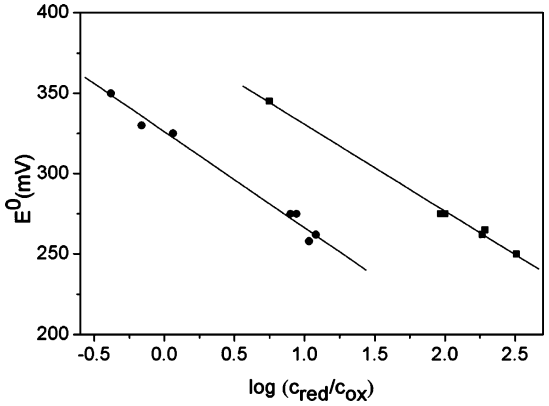

Figure 5. Nernst plots for the redox processes of immobilized QO. Circles: heme *a*. Squares: heme a_3. The relative concentrations of the species were determined by component analysis of the potential-dependent SERR spectra (see text).

compared to that of type A heme−copper oxygen reductases. In the fully oxidized state of mammalian Cox, for example, the midpoint potentials of hemes *a* and a_3 are ca. 390 and 200 mV, respectively, which, in principle, would correspond to an uphill electron transfer process. However, the midpoint potentials of the four redox centers in Cox are strongly modulated by their oxidation states and the protonation state of redox Bohr sites.[7,42,43] The underlying molecular mechanism that ensures an efficient downhill electron transfer cascade coupled to uphill proton translocation is still a matter of debate, but essentially consists of a complex network of cooperativities, including Coulombic interactions and mechano-chemical components.[7,42,43] The complexity of the process is reflected by the redox titration curves of hemes *a* and a_3 that show strong deviations from a linear Nernst behavior,[13] in contrast to the present results for QO.

Conclusions

The present results suggest a substantially different mechanistic scheme for the electroprotonic energy transduction in QO with respect to type A (mitochondrial-like) aa_3 enzymes. In both cases, the free energy provided by downhill electron transfer reactions is utilized for vectorial proton transport. For type A enzymes, the exergonicity of the electron transfer cascade is facilitated by a sophisticated network of cooperativities. In contrast, downhill electron transfer in QO is already guaranteed by the inversion of the intrinsic midpoint potentials of hemes *a* and a_3, such that, from this point of view, modulation by cooperativity effects is not required. In agreement with this interpretation, the two hemes can be treated as independent redox couples with no indication for substantial electrostatic interactions.

An inversion of the midpoint potentials with respect to type A enzymes has also been observed for the type B ba_3 oxygen reductase of another extremophyle organism, *Thermus thermophilus*.[44] Whether this is a phylogenetic characteristic of the type B enzymes or originates from an adaptation response specific to these two extremophyle organisms remains an interesting open question.

The dynamics of the redox-linked conformational transitions that occur at the level of the active site of QO is sensitively affected by the interfacial electric field, which is comparable in magnitude to the values reported for biological membranes. Electric field or membrane potential control of charge transfer reactions and coupled processes have also been observed for Cox,[45] Cyt-c,[21] photosynthetic reaction centers,[46] bacteriorhodopsin,[47] and sensory rhodopsin II.[48] Therefore, we propose that electric fields may play an active role in the regulation of aerobic respiration and of charge transfer processes at membranes in general.

Acknowledgment. The financial support by the FCT (POCTI-BIO-43105-2001 and POCTI-BME-45122-2002) and the DFG (Sfb498, A8) is gratefully acknowledged. S.T. and M.M.P. are recipients of FCT fellowships.

JA052921L

(42) Brunori, M.; Giuffre, A.; Sarti, P. *J. Inorg. Biochem.* **2005**, *99*, 324−336.
(43) Wikström, M. *Biochim. Biophys. Acta* **2004**, *1655*, 241−247.
(44) Hellwig, P.; Soulimane, T.; Buse, G.; Mäntele, W. *Biochemistry* **1999**, *38*, 9648−9658.
(45) Gregory, L.; Ferguson-Miller, S. *Biochemistry* **1989**, *28*, 2655−2662.
(46) Lao, K. Q.; Franzen, S.; Steffen, M.; Lambright, D.; Stanley, R.; Boxer, S. G. *Chem. Phys.* **1995**, *197*, 259−275.
(47) Nagel, G.; Kelety, B.; Mockel, B.; Buldt, G.; Bamberg, E. *Biophys. J.* **1998**, *73*, 403−412.
(48) Rivas, L.; Hippler-Mreyen, S.; Engelhard, M.; Hildebrant, P. *Biophys. J.* **2003**, *84*, 3864−3873.